ACS APPLIED MATERIALS & INTERFACES

Research Article

Cite This: ACS Appl. Mater. Interfaces 2017, 9, 38211-38221

www.acsami.org

Highly Specific Binding on Antifouling Zwitterionic Polymer-Coated Microbeads as Measured by Flow Cytometry

Esther van Andel,[†,‡] Ian de Bus,[†] Edwin J. Tijhaar,[‡] Maarten M. J. Smulders,[†] Huub F. J. Savelkoul,[*,‡] and Han Zuilhof[*,†,§,∥]

[†]Laboratory of Organic Chemistry, Wageningen University, Stippeneng 4, 6708 WE Wageningen, The Netherlands

[‡]Cell Biology and Immunology Group, Wageningen University, De Elst 1, 6709 PG Wageningen, The Netherlands

[§]School of Pharmaceutical Sciences and Technology, Tianjin University, 92 Weijin Road, Tianjin 300072, People's Republic of China

[∥]Department of Chemical and Materials Chemistry, King Abdulaziz University, Jeddah 21589, Saudi Arabia

Supporting Information

ABSTRACT: Micron- and nano-sized particles are extensively used in various biomedical applications. However, their performance is often drastically hampered by the nonspecific adsorption of biomolecules, a process called biofouling, which can cause false-positive and false-negative outcomes in diagnostic tests. Although antifouling coatings have been extensively studied on flat surfaces, their use on micro- and nanoparticles remains largely unexplored, despite the widespread experimental (specifically, clinical) uncertainties that arise because of biofouling. Here, we describe the preparation of magnetic micron-sized beads coated with zwitterionic sulfobetaine polymer brushes that display strong antifouling characteristics. These coated beads can then be equipped with recognition elements of choice, to enable the specific binding of target molecules. First, we present a proof of principle with biotin-functionalized beads that are able to specifically bind fluorescently labeled streptavidin from a complex mixture of serum proteins. Moreover, we show the versatility of the method by demonstrating that it is also possible to functionalize the beads with mannose moieties to specifically bind the carbohydrate-binding protein concanavalin A. Flow cytometry was used to show that thus-modified beads only bind specifically targeted proteins, with minimal/near-zero nonspecific protein adsorption from other proteins that are present. These antifouling zwitterionic polymer-coated beads, therefore, provide a significant advancement for the many bead-based diagnostic and other biosensing applications that require stringent antifouling conditions.

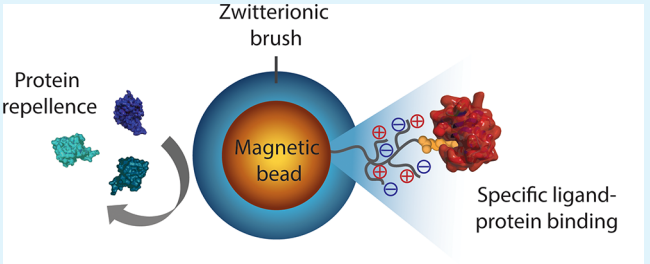

KEYWORDS: *antifouling, zwitterionic polymer, microbead, flow cytometry, sulfobetaine, biosensing*

INTRODUCTION

Nano- and micron-sized particles have emerged as powerful platforms for many biomedical applications,[1−5] including imaging, drug delivery, cell sorting as well as for biomolecule detection, separation, and quantification. Especially, magnetic particles have been shown to be highly valuable because of their quick and easy separation from their sample matrix, simply by applying an external magnetic field.[1,2] Despite their frequent use in biomedical applications, these particles often suffer from the nonspecific adsorption of biomolecules such as cells and proteins, a process called biofouling.[5−7] In sensing applications, fouling of the particle surface hampers the sensitivity and selectivity toward its target, leading to deteriorated signal-to-noise ratios and resulting in false-positive or false-negative outcomes.[8,9] To improve the performance of these particles, it is crucial to incorporate antifouling coatings on the surface of the particles to prevent biofouling.

Antifouling coatings have been extensively studied, yet mainly on flat surfaces.[10,11] Oligo(ethylene glycol)- and poly(ethylene glycol) (PEG)-based materials are the most studied and frequently used antifouling coatings.[12,13] However, PEG-based materials are prone to autoxidation, which limits their use for applications requiring long-term stability.[14,15] Moreover, their performance is limited when exposed to complex, real-life biological fluids,[16] that is, the conditions typically observed in biomedical applications. Polymeric zwitterionic materials have been brought forward as excellent alternatives because of their high protein resistance in complex protein mixtures such as blood plasma and serum,[16,17] combined with their long-term stability in aqueous solutions[18] and biocompatibility.[19] *Grafting-from* polymerization via atom transfer radical polymerization (ATRP),[20] that is, growing polymer brushes from a surface, has become the method of choice for the preparation of zwitterionic coatings. It yields highly antifouling, densely packed coatings with tunable thicknesses.[21] Carboxybetaines (CBs) and sulfobetaines (SBs)

Received: July 5, 2017
Accepted: October 10, 2017
Published: October 24, 2017

DOI: 10.1021/acsami.7b09725
ACS Appl. Mater. Interfaces 2017, 9, 38211−38221

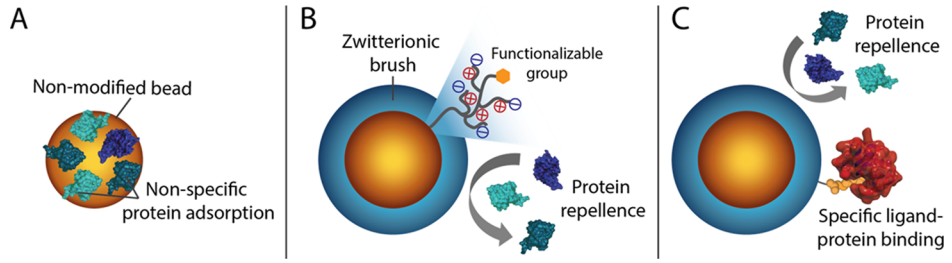

Figure 1. Schematic representation of (A) a nonmodified bead with a significant amount of nonspecifically bound proteins, (B) an antifouling zwitterionic polymer-coated bead that repels all biomolecules (before functionalization with a biorecognition unit), and (C) an antifouling polymer-coated bead equipped with a recognition unit that specifically binds its target while still being able to repel all unwanted proteins.

have become the zwitterionic monomers of choice because of their commercial availability, straightforward synthesis, and outstanding performance.[22,23]

Although antifouling coatings have been widely investigated on flat surfaces, their use in nano- and micron-sized particles remains largely unexplored. Apart from a small number of studies describing the use of PEG-derived materials[9,24] or zwitterionic coatings prepared by a *grafting-to* method with modified poly(acrylic acid),[8,25] only two preliminary studies by Jia et al.[6] and Yang et al.[7] describe ATRP-prepared zwitterionic CB polymer-coated nanoparticles for sensing purposes. However, both these studies lack not only a sophisticated biological read-out system that allows for the discrimination between specific and nonspecific protein binding, but also the ability to perform analysis on single beads rather than on the bulk. We anticipated, therefore, that a sensing platform based on ATRP-prepared antifouling beads that can be analyzed by flow cytometry would be highly valuable. Flow cytometry is indispensable in biomedical research and is routinely used in clinical diagnostics, for example, to monitor the course and treatment of HIV infections and to determine the prognoses and optimal treatment for several types of cancers.[26−28] Moreover, flow cytometry allows for the simultaneous and multiparametric analysis of hundreds to thousands of cells or micron-sized particles per second,[26] which makes it a very powerful and frequently used read-out system. Herein, we demonstrate that flow cytometry is also an excellent technique to study specific versus nonspecific binding on micron-sized particles.

Here, we develop a route toward generically antifouling zwitterionic SB polymer (pSB)-coated beads that still can bind a specific protein of interest (see Figure 1). With this aim, magnetic amine-functionalized beads (Dynabeads; 2.8 μm diameter) were selected as the starting material. These beads are compatible with flow cytometry instruments, stable in both aqueous and organic solvents, and can be easily separated from solvents/reactants because of their magnetic core. Top functionalization of the pSB-coated beads with biotin or mannose allowed for the specific binding of streptavidin or concanavalin A (ConA), respectively, from complex biological media. These pSB-coated beads showed excellent antifouling properties combined with a selective binding of the protein of interest. This platform, therefore, shows great potential for the development of a range of bioassays that require ultralow biofouling conditions.

MATERIALS AND METHODS

Materials. All chemicals and solvents were used without further purification. α-Bromoisobutyryl bromide (98%), trimethylamine (BioUltra, ≥99.5%), copper(I) chloride (≥99%), copper(II) chloride (97%), sodium azide (BioUltra, ≥99.5%), dimethyl sulfoxide (DMSO) (anhydrous, ≥99.9%), acetone semiconductor grade (VLSI PURANAL Honeywell 17617), tris(3-hydroxypropyltriazolylmethyl)amine (THPTA; 95%), copper(II) sulfate pentahydrate (98%), and (+)-sodium L-ascorbate (BioXtra, ≥99.0%) were purchased from Sigma-Aldrich. Dimethylformamide (DMF) for peptide synthesis (99.8%) and monopropargylamine (≥99%) were obtained from Acros Organics, 2,2′-bipyridine (98%) from Alfa Aesar, isopropanol (high performance liquid chromatography) from BioSolve, 2,2,3,3,4,4,4-heptafluorobutylamine (97%) from Fisher Scientific, dichloromethane (DCM) from VWR International S.A.S., and 8-(+)-biotinylamino-3,6-dioxa-octyl(1*R*,8*S*,9*S*)-bicyclo[6.1.0]non-4-yn-9-ylmethyl carbamate (BCN-biotin) from Synaffix. Milli-Q was produced with a Milli-Q Integral 3 system (Millipore).

Dynabeads (Dynabeads M-270 amine; 2.8 μm diameter) and ConA-Alexa Fluor 647 conjugate (ConA-AF647) were purchased from Invitrogen Life Technologies. Bovine serum albumin-Alexa Fluor 488 conjugate (BSA-AF488) and EZ-Link Sulfo-NHS-LC-Biotin were obtained from Thermo Fisher and streptavidin-phycoerythrin (Strep-PE) conjugate from eBioscience. PD10 desalting columns were purchased from GE Healthcare, streptavidin-poly-HRP80 (Strep-HRP) (1 mg/mL) from Stereospecific Detection Technologies, and Enhanced K-Blue tetramethylbenzidine (TMB) substrate from Neogen. Bovine blood sample collection was approved by the Board on Animal Ethics and Experiments from Wageningen University (DEC number: 2014005.b).

Synthesis. The synthesis of all noncommercially available compounds has been previously described, as detailed below. The 3-((3-methacrylamidopropyl)dimethylammonio)propane-1-sulfonate (SB) monomer and BCN-2,2,2,-trifluoroacetate (BCN-CF_3) were described by Lange et al.,[29] 1-(11-azidoundecanyl)-α-D-mannopyranoside (mannose-C_{11}-azide) by Debrassi et al.,[30] and 13,13,14,14,15,15,16,16,16-nonafluorohexadec-1-yne (F_9-alkyne) by Pujari et al.[31]

Bead Handling. During all collection and washing steps, beads were collected using a magnetic stand (Promega) which allows for quick and easy separation of the beads from solvent and reactants. All reactions described below are based on 100 μL (corresponding to approximately 3 mg beads, containing ~2×10^8 beads) of the original nonmodified bead suspension as provided by the manufacturer. If no bead volume is mentioned, solvent (Milli-Q) was removed, and the beads were resuspended in the solvent of choice. In all cases, unless stated otherwise, 2 mL Eppendorf tubes were used for bead modifications. After each reaction, the beads were stored in a small amount of Milli-Q at 4 °C until further use.

Initiator Attachment. The bromo-initiator was incorporated by first drying 100 μL of amine-terminated Dynabeads in a vacuum oven at 50 °C for 2 h. The dried beads were resuspended in 1.25 mL of dry DCM and transferred to a glass tube with screw cap connection. The bead suspension was bubbled with argon while 700 μL of triethylamine and 370 μL (3 mmol) of α-bromoisobutyryl bromide were added. The glass tube was closed with a screw cap, covered with aluminum foil and placed for 3 h on an end-over-end shaker at room temperature (RT). The beads were washed with copious amounts of DCM to dissolve any precipitate that might have formed. The beads

DOI: 10.1021/acsami.7b09725
ACS Appl. Mater. Interfaces 2017, 9, 38211−38221

were transferred to an Eppendorf tube and washed twice with isopropanol and twice with Milli-Q.

Surface-Initiated Polymerization. Surface-initiated ATRP was performed as previously described[29] with slight modifications. Solvents were degassed by sonication (5 min) and argon bubbling for 30 min. Reactants were kept under argon atmosphere during all steps. A mixture of 41.0 mg of 2,2-bipyridyl and 12.1 mg of a Cu(I)Cl/Cu(II)Cl_2 (9/1) mixture was prepared in a glovebox under argon atmosphere, dissolved in 5.25 mL of isopropanol/Milli-Q (1/4), and stirred for 15 min. Using argon-flushed needles, 2 mL of the resulting brown solution (containing 0.1 mmol (1 equiv) bipyridyl and 0.045 mmol (0.45 equiv) copper mix) was then transferred to a Schlenk flask containing 731 mg (2.5 mmol, 25 equiv) of the 3-((3-methacrylamidopropyl)dimethylammonio)propane-1-sulfonate (SB) monomer. This mixture was stirred for 15 min or until full solubilization of the SB monomer. Meanwhile, the required amount of initiator-functionalized beads was bubbled with argon for 10 min in a total volume of 1 mL of degassed isopropanol/Milli-Q (1/4). The monomer-containing solution was then transferred (2 mL) to the beads to a final volume of 3 mL. The polymerization reaction was carried out for 1 min at RT, while shaking by hand to ensure proper dispersion of the beads. The reaction was stopped by pouring the solution into an Erlenmeyer flask and adding Milli-Q while swirling, until the solution turned blue. The blue color indicates the oxidation, and thereby inactivation, of the copper catalyst, which hence stops the polymerization reaction. The pSB-coated beads were collected using a magnet and washed two times with isopropanol/Milli-Q (1/4), twice with phosphate-buffered saline (PBS), and twice with Milli-Q.

Top-Functionalization of Polymer-Coated Beads. *Fluorobutylamine.*[32] Substitution of the terminal halogen with a fluorine-containing molecule for X-ray photoelectron spectroscopy (XPS) analysis was achieved by immersing pSB-coated beads in a 2 M solution of 2,2,3,3,4,4,4-heptafluorobutylamine in DMF (290 μL of the fluoroamine and 210 μL of DMF) in a small glass tube closed with a screw cap. The glass tube was covered with aluminum foil and placed in an oil bath at 65 °C; the beads were allowed to react for 16 h. The next day, the reaction tube was cooled to RT, and the beads were transferred to an Eppendorf tube and washed twice with DMF, twice with PBS, and twice with Milli-Q.

Azide Introduction.[33] Azide moieties were introduced on pSB-coated beads by immersing the beads in 1 mL of a 0.5 M solution of sodium azide in PBS in an aluminum foil-covered Eppendorf tube. The tube was placed on an end-over-end shaker for 16 h at RT. The pSB-azide beads were washed three times with PBS and twice with Milli-Q.

Alkyne Introduction. Alkynes were introduced using a 2 M solution of propargylamine (128 μL for 1 mL) in PBS. The solution was added to the pSB beads and reacted in an Eppendorf tube covered with aluminum foil overnight on an end-over-end shaker at RT. The pSB-alkyne beads were washed three times with PBS and twice with Milli-Q.

Click Chemistry: Brush Functionalization. *Brush Functionalization Using Strain-Promoted Azide–Alkyne Cycloaddition (SPAAC).*[29] For the reaction of azide-functionalized polymer brush-coated beads with BCN-biotin or BCN-CF_3, first a 40 mM stock solution of the BCN compound was prepared in anhydrous DMSO (stored at −20 °C). To an Eppendorf tube, 100 μL of this solution and 100 μL of pSB-azide beads, suspended in Milli-Q, were added to a final BCN concentration of 20 mM. The tube was placed on an end-over-end shaker overnight at RT; the beads were subsequently washed two times with DMSO, twice with PBS, and twice with Milli-Q.

Brush Functionalization Using Copper-Catalyzed Azide–Alkyne Cycloaddition (CuAAC). For the click reaction on azide-containing beads with 13,13,14,14,15,15,16,16,16-nonafluorohexadec-1-yne (F_9-alkyne), two stock solutions were prepared: a 10 mL aqueous solution containing 2.5 mM $CuSO_4{\cdot}5H_2O$ (6.24 mg) and 50 mM (+)-sodium L-ascorbate (99.0 mg), and a 1 mL solution of 12.5 mM THPTA (5.43 mg) and 100 mM of the F_9-alkyne (38.4 mg) in DMSO. Each solution (100 μL) was added to an Eppendorf tube, and 10 times diluted by adding the alkyne/azide-functionalized beads suspended in 800 μL of DMSO/Milli-Q (1/1). This resulted in the following final concentrations: 0.25 mM $CuSO_4$, 5 mM sodium ascorbate, 1.25 mM THPTA, and 10 mM of the alkyne. For an effective click reaction of mannose-C_{11}-azide with alkyne-terminated beads, the above protocol had to be modified, which was done via the guidelines provided by Hong et al.[34] Three stock solutions were prepared: a 10 mL aqueous PBS solution containing 1 mM $CuSO_4{\cdot}5H_2O$ (2.49 mg) and 5 mM THPTA (21.7 mg), a 10 mL aqueous PBS solution containing 12.5 mM (+)-sodium L-ascorbate (24.8 mg), and 2 mL containing 5 mM mannose-C_{11}-azide (3.8 mg). The following was added, in this order, to an Eppendorf tube: 400 μL of DMSO, 200 μL of PBS containing the alkyne-terminated beads, 100 μL of the $CuSO_4$/THPTA solution, 100 μL of the mannose-C_{11}-azide solution, and finally 200 μL of the sodium ascorbate solution to initiate the reaction. The final concentrations of the reactants: 100 μM $CuSO_4$, 500 μM THPTA, 2.5 mM ascorbate, and 500 μM of mannose-C_{11}-azide.

The CuAAc reactions were performed overnight (16 h) on an end-over-end shaker at RT. The beads were washed twice with DMSO, DMSO/Milli-Q (1/1), PBS and Milli-Q.

Bead Characterization. *XPS.* XPS samples were prepared by concentrating the beads (in Milli-Q) and dropcasting 10 μL of this suspension onto a piece of Si(111) (Siltronix, N-type, phosphorus doped), which was cleaned by rinsing and sonicating for 5 min in semiconductor grade acetone followed by oxygen plasma treatment (Diener electronic, Femto A) for 5 min at 50% power. The dropcasted samples were subsequently dried in a vacuum oven at 50 °C for at least 2 h before XPS measurements were started. XPS spectra were obtained using a JPS-9200 photoelectron spectrometer (JEOL, Japan) with monochromatic Al Kα X-ray radiation at 12 kV and 20 mA. The obtained spectra were analyzed using CASA XPS software (version 2.3.16 PR 1.6).

Fourier Transform Infrared Spectroscopy. Fourier transform infrared spectroscopy (FT-IR) samples were prepared by drying ~10 μL of Milli-Q-washed beads in a vacuum oven at 50 °C for at least 2 h. The dried beads were transferred to a small piece of gold-coated Si(111) and subsequently measured by a Bruker Tensor 27 IR spectrometer, connected to a Bruker HYPERION 2000 IR microscope with a liquid nitrogen-cooled mercury cadmium telluride detector. Both apparatuses were controlled using Bruker's OPUS software. The microscope was used to select an area with a sufficient amount of beads and a proper background position. For each background and sample measurement 128 scans were taken.

Flow Cytometry. Beads were suspended in 0.5 mL of PBS and shortly vortexed before measuring with a BD FACSCanto II (BD Biosciences) flow cytometer. Per sample, 10.000 single beads were measured; for the gating strategy that was used, see the Supporting Information. Data analysis was performed using FlowJo software V10.

Confocal Microscopy. Fluorescence images were taken using a confocal laser scanning microscope (Leica TCS SP8X system), equipped with a 63×/1.2NA water immersion objective. BSA-AF488 and Strep-PE were excited using a white light pulsed (repetition rate 40 MHz) laser selecting the 488-laser line and 561-laser line, respectively. Fluorescence emission was collected between 500 and 530 nm for AF488, and the PE fluorescence emission was selected by measuring between 570 and 610 nm. Images were captured in a photon-counting mode, accumulating photons over 10 frames. The pinhole was set to 0.39 Airy units, and an optical zoom of 8.00 was used to capture the images. Confocal images were analyzed with the LAS AF Lite (version 2.6.0) software.

Antifouling and Specific Binding Studies. *Serum Labeling.* Bovine blood serum samples were obtained from healthy cows via coccygeal vein sampling. Serum was collected using VACUETTE tubes (4 mL Z Serum Separator Clot Activator 13 × 75 gold cap-gold ring, PREMIUM) from Greiner Bio-One. Serum from 3 individual cows was pooled and heated for 30 min at 56 °C in a water bath (to inactivate complement) and stored at −20 °C. Labeling of serum proteins was performed using an AnaTag HiLyte Fluor 488 microscale protein labeling kit (AnaSpec, Inc.) according to the manufacturer's instructions using 84 μL of serum per batch. After labeling, the samples were concentrated using Amicon Ultra-4 centrifugal filter tubes (Millipore BV). The filters were first washed with PBS, labeled

DOI: 10.1021/acsami.7b09725
ACS Appl. Mater. Interfaces 2017, 9, 38211−38221

Scheme 1. Overview of Chemical Modifications on Amine-Terminated Beads to Yield Functionalized Antifouling pSB-Coated Beads[a]

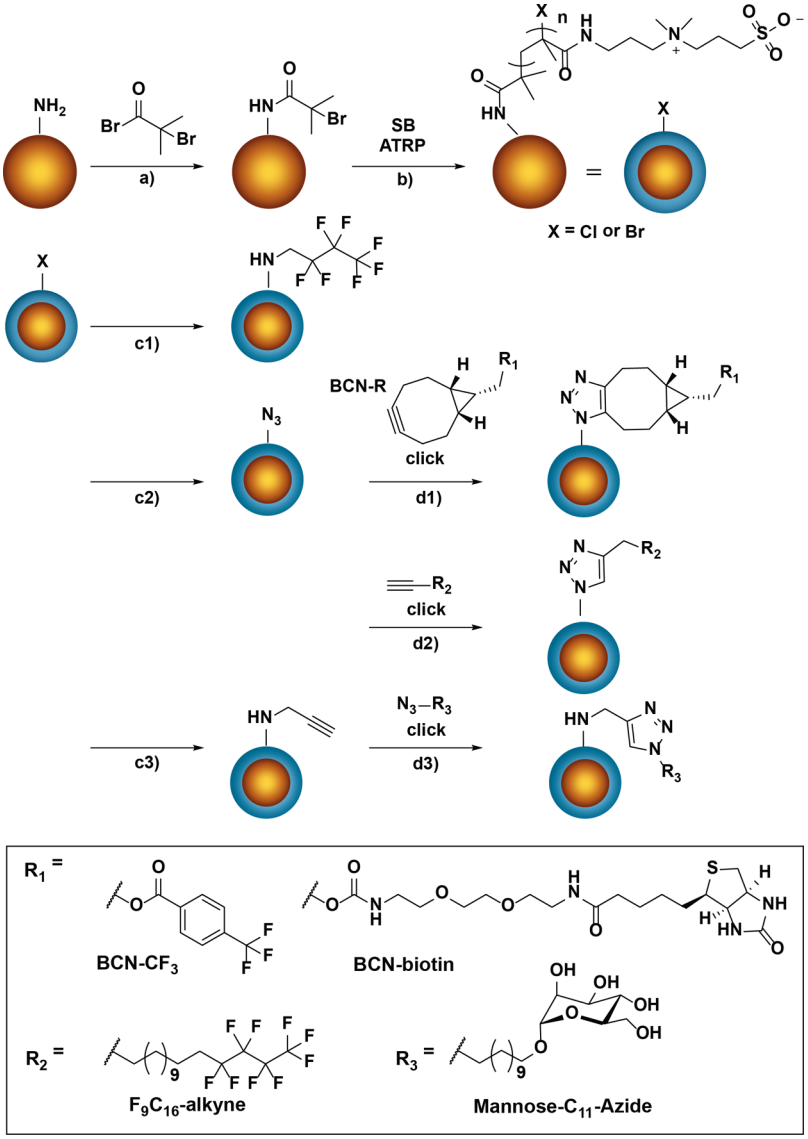

[a]The reaction conditions represented by the arrows are as follows: (a) 2.4 M α-bromoisobutyryl bromide, DCM, Et_3N, RT, 3 h. (b) SB, Cu(I)/Cu(II) (9/1), bipyridine, isopropanol/Milli-Q (1/4), RT, 1 min. (c1) 2 M heptafluorobutylamine, DMF, 65 °C, 16 h. (c2) 0.5 M NaN_3, PBS, RT, 16 h. (c3) 2 M propargylamine, PBS, RT, 16 h. (d1) SPAAC, 20 mM BCN-R_1, DMSO/Milli-Q (1/1), RT, 16 h. (d2) CuAAC, 10 mM F_9-alkyne, 0.25 mM $CuSO_4$, 5 mM Na ascorbate, 1.25 mM THPTA, DMSO/Milli-Q (1/1), RT, 16 h. (d3) CuAAC, 500 μM mannose-C_{11}-azide, 100 μM $CuSO_4$, 2.5 mM sodium ascorbate, 500 μM THPTA, DMSO/Milli-Q (1/1), RT, 16 h.

serum was added, and the tubes were centrifuged for 35 min at 3363*g* at 4 °C. The obtained concentrated labeled serum had a final concentration of 21.2 mg/mL. From this, a 10% serum-HLF488 solution was reconstituted with a concentration of 6 mg/mL.

Serum Biotinylation. The same pooled cow's serum that was used for the HiLyte Fluor 488 serum labeling was also used for biotinylation. Serum proteins were biotinylated using an EZ-Link Sulfo-NHS-LC-Biotin reagent, using the manufacturer's instructions. To a 2 mL Eppendorf tube, 60 mg of serum proteins and 429 μL of a 100 mM sulfo-NHS-biotin solution (in PBS) were added to a final volume of 2 mL. Assuming that all proteins in serum have a molecular weight of 70 kDa, 50 equivalents of sulfo-NHS-biotin was used relative to the amount of proteins. The reaction was carried out at RT for 60 min. Nonbound reagents were removed by using a desalting PD-10 column (Sephadex), following the manufacturer's gravitation protocol with PBS as the eluent. The concentration of the obtained biotinylated serum (serum-biotin) was adjusted to a 10% serum solution (6 mg/mL).

Protein Dilution Series. Two-fold serial dilutions (200 μL each, in Eppendorf tubes) were prepared from the following protein solutions: 1 mg/mL bovine serum albumin-Alexa Fluor 488 conjugate (BSA-AF488), 100 μg/mL Strep-PE conjugate, and 10% HiLyte Fluor 488-labeled serum (serum-HLF488, ~6 mg/mL). To each dilution, either 2×10^6 nonmodified beads or 2×10^6 pSB beads were added. Beads were counted using a cell-counting chamber to ensure equal amounts of beads. Each Eppendorf tube was wrapped with aluminum foil to avoid degradation of the fluorophore and placed on an end-over-end shaker for 1 h at RT. The beads were washed three times with PBS and analyzed by flow cytometry for their fluorescence.

Quantification by ELISA. Nonmodified beads and pSB-coated beads (10×10^6 beads per sample, counted using a cell-counting chamber) were incubated with serum-biotin, washed three times with PBS, followed by incubation with horseradish peroxidase-conjugated

DOI: 10.1021/acsami.7b09725
ACS Appl. Mater. Interfaces 2017, 9, 38211−38221

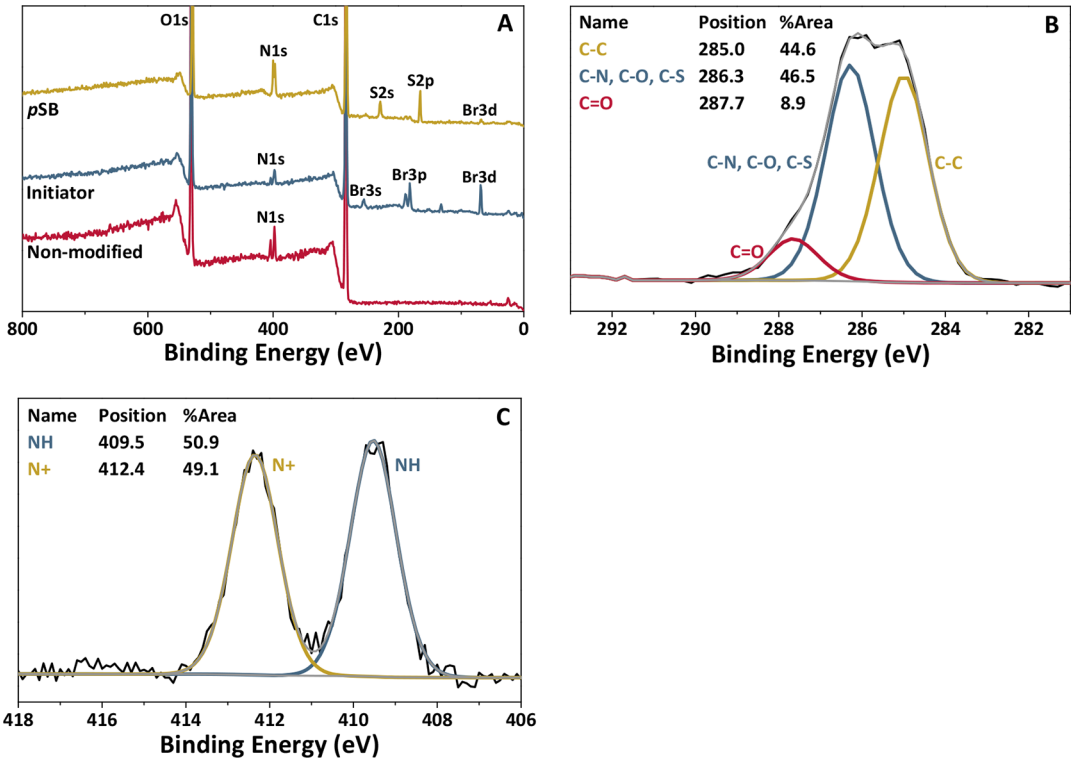

Figure 2. (A) XPS wide scans of nonmodified beads, initiator-functionalized and pSB polymer-coated beads. (B) XPS N 1s and (C) C 1s narrow scans of pSB-coated beads. The spectra show the successful growth of zwitterionic polymer brushes from the beads.

streptavidin (Strep-HRP, 1:100 dilution from purchased stock solution) or directly with Strep-HRP. Beads were washed five times with PBS, transferred to a new Eppendorf tube, and washed an additional 5 times to ensure that all nonbound Strep-HRP had been removed. Twofold serial dilutions (1.7 serial dilutions for the Serum-biotin samples) were made of the bead samples, with each a final volume of 50 μL. To each dilution, 200 μL TMB solution was added, followed by 100 μL 4% HCl to stop the enzymatic reaction. The optical density was measured in a 96-well plate at 450 nm and subtracted by the absorbance measured at 620 nm to correct for irregularities within the plastic.

Protein Binding Studies. For each sample, 100 μL of protein solution (or PBS only) was prepared into 2 mL Eppendorf tubes prior to the addition of 2 μL of beads. Single protein solutions or protein mixtures were prepared in the following concentrations: 50 μg/mL Strep-PE, 50 μg/mL ConA-AF647 conjugate, 0.5 mg/mL BSA-AF488, and 10% Serum-HLF488 (~6 mg/mL). PBS buffer with additional $CaCl_2$ (1 mM) was used for each sample that contained ConA-AF647. After adding the coated beads to the protein solutions, the tubes were covered with aluminum foil and placed on an end-over-end shaker for 1 h at RT. The beads were then washed three times with PBS and analyzed by either flow cytometry or confocal microscopy.

RESULTS AND DISCUSSION

Coating Beads with Zwitterionic Polymer Brushes. Our first step in the surface modification toward an antifouling bead with installed recognition elements is the introduction of an ATRP initiator, which could be achieved straightforwardly by reacting the amino groups of the beads with the acid bromide group of bromoisobutyryl bromide (Scheme 1, route a). Successful incorporation of the initiator was confirmed by XPS analysis (Figure 2), which showed the appearance of distinctive peaks characteristic of the element bromide (see the Supporting Information Figure S2 for XPS narrow scans). Moreover, FT-IR spectroscopy demonstrated the appearance of a carbonyl peak at 1732 cm^{-1} (see the Supporting Information, Figure S9). From the installed initiator, zwitterionic polymer brushes were grown via ATRP,[20] based on our previously described procedure.[29] Polymer brushes were grown using the zwitterionic SB monomer to yield pSB-coated beads (Scheme 1, route b).

The beads were analyzed by XPS (Figure 2), and the growth of the zwitterionic coating was confirmed by the appearance of the two sulfur peaks, S 2s (232.0 eV) and S 2p (168.0 eV), originating from the negatively charged sulfonate group. In addition, the XPS N 1s spectrum shows the expected characteristic 1:1 ratio of the amide (409.5 eV) and ammonium (412.4 eV) peaks. The equal ratio of these two peaks implies that the signal of the underlying bead can no longer be detected, which indicates a sufficiently thick polymer layer (clearly in excess of ~10 nm) that is required for a good antifouling performance.[18] The XPS C 1s spectrum displays three distinguishable peaks corresponding to the C−C carbon atoms at 285.0 eV, the carbon atoms next to a heteroatom (C−O, C−N, and C−S) at 286.3 eV and a peak corresponding to the carbonyl of the amide bond at 287.7 eV. Reassuringly, the XPS wide scan, N 1s, and C 1s spectra of the polymer brush-coated beads are practically identical to previously obtained spectra for flat surfaces.[18,29] It is worthwhile to mention the small, remaining Br peak in the XPS wide scan of the pSB-coated beads that can still be discerned in the top spectrum of Figure 2A. This peak can be attributed to the terminal bromides that are retained at the polymer chain ends after ATRP. As described below, these bromides offer a useful functional handle to introduce specific recognition elements.

Antifouling Properties of pSB-Coated Beads. Traditionally, antifouling properties of coated surfaces are evaluated by investigating the amount of nonspecifically bound proteins

DOI: 10.1021/acsami.7b09725
ACS Appl. Mater. Interfaces 2017, 9, 38211−38221

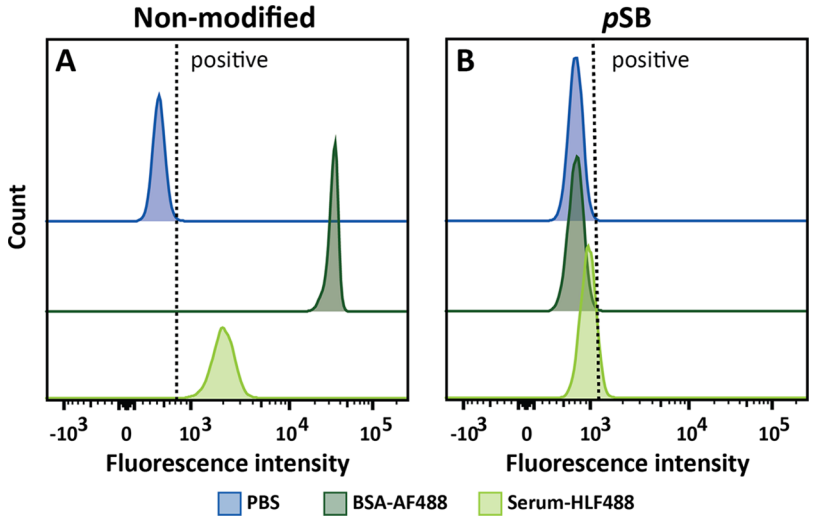

Figure 3. Representative flow cytometry data of (A) nonmodified and (B) pSB-coated beads incubated in either PBS or a protein solution containing BSA-AF488 (0.5 mg/mL) or serum-HLF488 (~6 mg/mL).

by using single-protein solutions of BSA, lysozyme, or fibrinogen.[12,13,22] More recently, it has become common practice to also include more complex biological media such as (diluted) blood plasma or serum. These more challenging conditions are typically used in biomedical applications and also turned out to be required to discriminate a high-efficacy antifouling surface from a moderate protein-repelling one.[35,36] For the evaluation of our pSB-coated beads, we therefore selected not only fluorescently labeled BSA (BSA-AF488, 0.5 mg/mL), but also included an in-house fluorescently labeled 10% cow's serum solution (serum-HLF488, ~6 mg/mL). The serum-HLF488 solution has a 12 times higher total protein concentration than the BSA-AF488 solution and also contains—aside from BSA—naturally occurring immunoglobulins and other serum proteins. Immunoglobulins, among other proteins such as human serum albumin and complement components, have been found on PEG-based surfaces that were exposed to human blood plasma,[37] and these types of proteins might therefore contribute to fouling of the beads presented in this study. The ability of the pSB-coated beads to repel all proteins in the used BSA and serum solutions was evaluated using flow cytometry. To this end, nonmodified beads and pSB-coated beads were incubated with either the BSA-AF488 or serum-HLF488 solution, and their fluorescence was measured after several washing steps. Per sample, 10 000 single beads were analyzed (see the Supporting Information, Figure S10, for the gating strategy and corresponding explanation on gating). Figure 3 shows the fluorescence of these beads, displayed as a histogram, showing the number of beads for a given fluorescent intensity of a selected fluorophore. Beads incubated in protein-free PBS are taken as the reference point, while beads with a higher fluorescence than the PBS beads (shifted to the right side of the gate, depicted as a dashed line in the histogram) are considered positive. Positive beads, therefore, indicate a significant increase in fluorescence, and therefore protein binding, as compared to the beads incubated in PBS only. A pronounced shift in fluorescence was observed (Figure 3A) for nonmodified beads that were incubated with either BSA-AF488 or serum-HLF488, indicating a significant amount of non-specifically bound proteins on these beads. In other words, unmodified beads suffer strongly from protein fouling. The pSB-coated beads, however, showed no difference in fluorescence between incubation in PBS or BSA-AF488 solution (as can be concluded from the identical blue and dark green peaks in Figure 3B), and only a minor increase when comparing the beads incubated with serum-HLF488 to beads incubated in PBS. This clearly demonstrates the excellent antifouling properties of the pSB-coated beads: the coating strongly reduces nonspecific binding of fluorescently labeled proteins, including proteins from a complex protein mixture.

The mean fluorescence intensity (MFI), normalized to the intensity of beads incubated in PBS, of nonspecifically bound proteins to either nonmodified or pSB-coated beads is summarized in Figure 4. Also, from these data, it is evident that nonmodified beads showed clear nonspecific protein adsorption when exposed to BSA-AF488 and serum-HLF488 solutions. Nonmodified beads also showed a clear increase in the nonspecific binding of fluorescently labeled ConA and a small but significant increase with labeled streptavidin [ConA-AF635 (MFI = 14053) and Strep-PE (MFI = 454), respectively], which are used for specific binding studies as described below. By contrast, pSB-coated beads displayed a nearly absent nonspecific binding of BSA-AF488, Strep-PE, and ConA-AF635. Only under the most challenging biofouling conditions that were studied, that is, incubation with serum-HL488, pSB-coated beads started to show a slight increase in protein adsorption (MFI = 272). However, this adsorption is only a fraction of the amount adsorbed on nonmodified beads (MFI = 1830). Finally, it is worthwhile to point out that inherent to the used method, the MFI of different fluorescently labeled protein solutions cannot be directly compared with respect to the amount of bound protein (see the Supporting Information).

To get further quantitative insight in the antifouling behavior of pSB-coated beads versus nonmodified beads, the beads were incubated with protein solutions at different concentrations. To this end, serial dilutions were prepared from BSA-AF488, Strep-PE, and serum-HLF488 solutions and added to the beads (see the Supporting Information, Figure S12). In all cases, pSB-coated beads performed evidently better than nonmodified beads. In fact, a direct comparison between nonmodified beads and pSB-coated beads that were incubated with either BSA-AF488 or Strep-PE was not feasible, as the amount of fouling on pSB beads was near zero. What can be concluded is that

DOI: 10.1021/acsami.7b09725
ACS Appl. Mater. Interfaces 2017, 9, 38211−38221

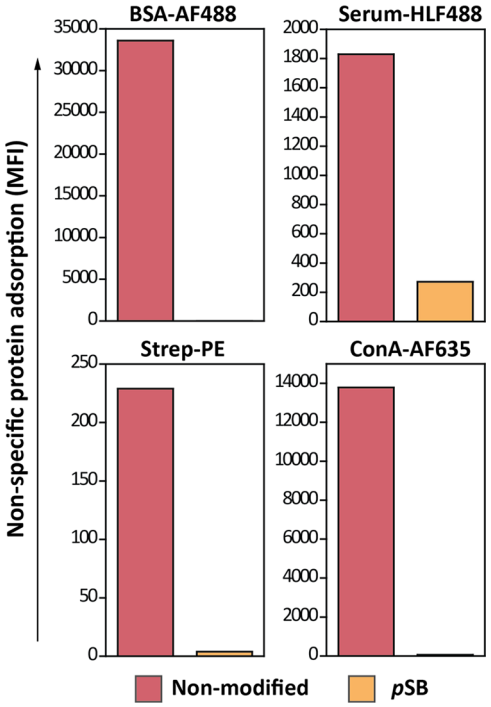

Figure 4. Representative flow cytometry data summarizing the MFI of nonmodified and pSB-coated beads incubated with PBS, BSA-AF488 (0.5 mg/mL), serum-HLF488 (10%, ~6 mg/mL), Strep-PE (50 μg/mL), or ConA-AF635 (50 μg/mL). MFI values are corrected for the autofluorescence of the beads by subtracting MFI values of their corresponding PBS samples; see the Supporting Information Table S1 for noncorrected values.

pSB-coated beads showed less fouling at the highest protein concentration than nonmodified beads do with a more than 500 times diluted protein sample. Nonmodified and pSB beads incubated with serum-HLF488 could be directly compared, as detectable fouling was also seen on pSB beads (for the four highest tested concentrations). Across these serum dilutions, ranging from 10 to 1.25%, the pSB-coated beads showed a factor 6−10 less fouling (MFI) than nonmodified beads. To verify these results, the amount of adsorbed protein on the beads was also assessed via a horseradish peroxidase (HRP) assay, similar to the well-known enzyme-linked immunosorbent assay (ELISA, see the Supporting Information, Figure S15). The beads were incubated with 10% biotinylated serum followed by Strep-HRP incubation or Strep-HRP directly. Serial dilutions were prepared from the bead samples, and the enzymatic (by HRP) conversion of TMB was measured at 450 nm. From the obtained titration curves, the relative amounts of bound Strep-HRP could be determined, and hence the amount of bound biotinylated serum, by comparing the number of beads necessary to obtain half of the maximum optical density (OD_{450} value). Almost no direct Strep-HRP adsorption could be detected—that is, in a solution in which Strep-HRP is the only protein, it basically does not absorb onto the pSB-coated beads—which makes a quantitative comparison with non-modified beads unfeasible. Only when using highly fouling serum, labeled with biotin and in the presence of Strep-HRP, fouling was seen on pSB beads, and thus a comparison could be made with nonmodified beads. Five to six times more pSB beads were needed to obtain an amount of signal similar to nonmodified beads. This indicates that under these conditions, pSB beads contain 5−6 times less adsorbed serum proteins than the nonmodified beads. The quantification by ELISA, therefore, corresponds well with the MFI ratio of 6 as obtained by flow cytometry for the same serum dilution (10%), confirming the power of flow cytometry as an accurate means to measure biofouling.

Functionalization of pSB-Coated Beads. Figure 3 shows the excellent antifouling properties of the pSB-coated beads. However, to use such beads for sensing purposes, they need to be combined with specific recognition elements. For this purpose, the terminal bromide that remains at the chain ends after ATRP polymerization can be used to incorporate biologically relevant molecules, as was already previously shown on pSB-coated silicon nitride surfaces.[38] To test the ability to modify pSB-coated beads in a similar fashion, several coupling reactions were performed which all aimed for the incorporation of fluorinated compounds—incorporation of fluorine facilitates the monitoring of the surface reactions by XPS because of the high sensitivity of this technique toward fluorine atoms. Initially, pSB-coated beads were reacted with a partially fluorinated hexadecylamine (Scheme 1, route c1). The appearance of a small, but distinct F 1s peak (686.0 eV) (Figure 5) and the concomitant disappearance of the Br 3d peak (see

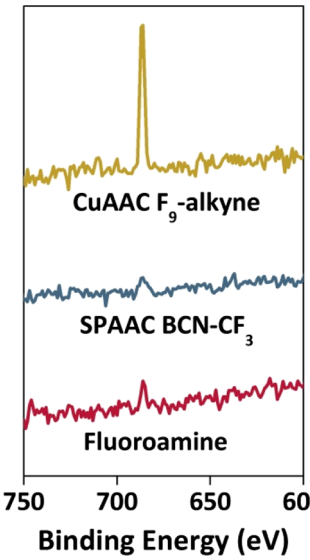

Figure 5. F 1s peaks from XPS wide scans obtained from pSB beads substituted with a heptafluorinated amine, pSB-azide beads functionalized with BCN-CF_3 via SPAAC, and pSB-azide beads functionalized with F_9-alkyne via CuAAC. The appearance of F 1s peaks in these XPS spectra indicates the successful functionalization of the polymer-coated beads with fluorinated model compounds.

the Supporting Information, Figure S5) in the XPS wide scan of these beads, indicated a successful substitution reaction, which thus confirms the availability of the terminal halide on the coated beads for surface reactions. To investigate the usability of pSB-coated beads for subsequent functionalization by click chemistry, the terminal bromides were first converted into azide moieties using sodium azide (Scheme 1, route c2).[33] The resulting pSB-azide beads were analyzed by FT-IR (see the Supporting Information, Figure S9), showing a clear azide signal at 2110 cm^{-1}. The incorporation of azides could be further confirmed by the additional peaks (apart from the amide and ammonium peak) in the XPS N 1s narrow scan (see the Supporting Information, Figure S4) that could be assigned to the azide moiety, similar to what was previously observed for

DOI: 10.1021/acsami.7b09725
ACS Appl. Mater. Interfaces 2017, 9, 38211−38221

azides within sulfobetaine brushes.[29] The pSB-azide beads were then functionalized via the widely used CuAAC[34] or SPAAC[29] click chemistry reactions using a fluorinated alkyne (F_9-alkyne, Scheme 1, route d2) or a CF_3-labeled bicyclooctyne (BCN-CF_3, Scheme 1, route d2), respectively. The CuAAC reaction showed the most evident F 1s peak (Figure 5). After correcting for the fact that the CuAAC reaction was performed with an alkyne containing nine fluorine atoms while with the SPAAC reaction only three fluorine atoms per molecule were incorporated, the CuAAC reaction was found to be more efficient than the SPAAC reaction (see the Supporting Information, Figures S6 and S7 for wide scans with atomic percentages) under the applied conditions.

The results described above demonstrate that the terminal halogen atoms that are present on the polymer chain ends after ATRP can indeed be used for further functionalization of the polymer-coated beads in a versatile manner either by directly substituting the halide with a functional amine or by first installing an azide moiety on the bead to introduce the appropriate (bio)molecule via click chemistry. As a result, a large variety of different (biological) relevant molecules can be incorporated onto the beads (of which two examples will be described below).

Specific Binding on Functionalized pSB Beads. To illustrate the ability to specifically bind a protein target onto the modified beads from a mixture of other proteins, pSB-azide beads were functionalized with BCN-biotin to bind streptavidin (Strep-PE). The specific and nonspecific binding of fluorescently labeled proteins on the thus-prepared pSB-biotin beads was first evaluated by confocal microscopy (Figure 6). To this end, nonmodified beads were incubated with either BSA-AF488 or Strep-PE, and pSB and pSB-biotin beads were incubated with a mixture of BSA-AF488 (0.5 mg/mL) and Strep-PE (50 μg/mL). The green channel, visualizing BSA-AF488, clearly shows nonspecific binding on nonmodified beads (Figure 6, left column, top panel). By contrast, no (nonspecific) BSA-AF488 binding is observed on pSB and pSB-biotin-coated beads (Figure 6, left column, middle, and bottom panel). In the red (PE) channel, no bound Strep-PE is visible except on pSB-biotin beads (Figure 6, right column, bottom panel), indicating solely specific binding of Strep-PE to the biotin moieties. Strep-PE did not show any nonspecific binding to nonmodified beads, which is consistent with the limited amount of bound streptavidin as measured by flow cytometry (see Figure 4). Interestingly, it was observed that nonspecific binding of BSA-AF488 was rather patchy (better visible in the Supporting Information, Figure S16), while the specific binding of Strep-PE was more evenly distributed. It has been shown before that serum albumin clusters are formed upon adsorption of this protein onto solid surfaces, especially at high protein concentrations that favor protein−protein interactions.[39,40] Whether the homogeneous distribution of streptavidin is a result of specific binding rather than nonspecific binding remains elusive.

The pSB-biotin beads were also analyzed by flow cytometry (Figure 7), including incubation under the more challenging conditions with serum-HLF488 solutions. Beads incubated with PBS were again used as a reference. The histograms for beads incubated with PBS (blue), BSA-AF488 (dark green), and serum-HLF488 (light green) are nearly identical (Figure 7A). That is, a shift in fluorescence was practically absent for pSB-biotin beads, irrespective of what protein or protein mixture it was incubated with. This indicates fully retained antifouling

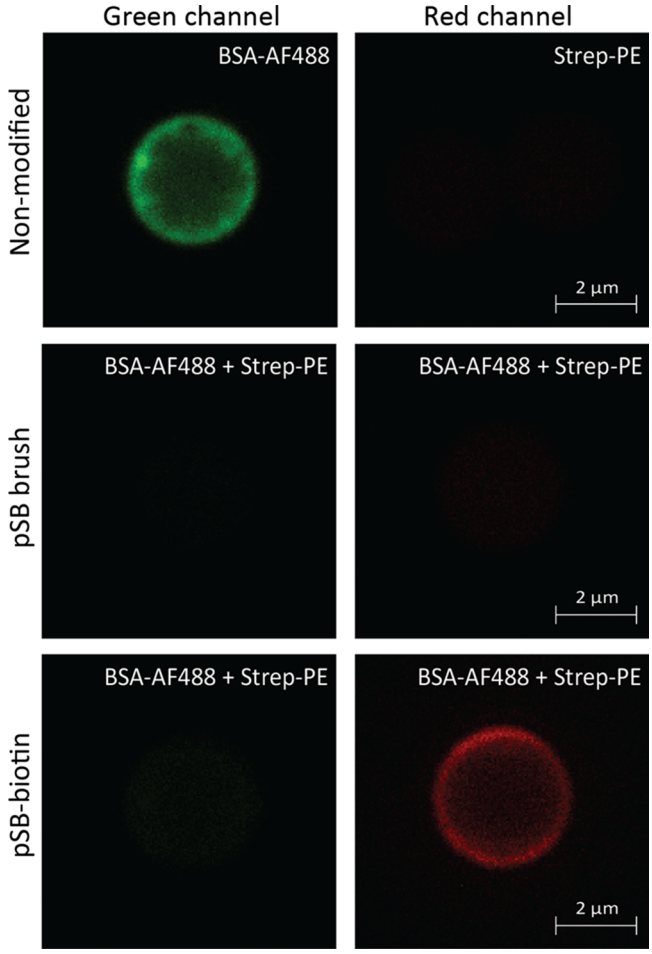

Figure 6. Confocal images of nonmodified, pSB-coated, and pSB-biotin beads incubated with BSA-AF488 (0.5 mg/mL) or Strep-PE (50 μg/mL) or a mixture of the two. The green channel shows the fluorescence as measured with a 488-laser line and a 500-531 nm band-pass filter, and the red channel shows the fluorescence as measured with a 561-laser line with a 570-610 nm band-pass filter.

properties of the beads after biotin functionalization. On the contrary, a clear shift in fluorescence was observed when the pSB-biotin beads were incubated with the target analyte, Strep-PE (Figure 7B), confirming the results obtained by confocal microscopy. The capacity to specifically bind Strep-PE was not hampered by the presence of a complex mixture of other proteins; as in Figure 7B, the Strep-PE peak for beads incubated with serum-HLF488 (magenta) is identical—both in peak width and peak position—to the peak of beads incubated with BSA-AF488 (orange). The relative sharpness of the peaks, as compared to beads in PBS, indicates the homogeneous functionalization of the beads with biotin and the subsequent binding of Strep-PE. After incubation with higher streptavidin concentrations, the fluorescence intensity of bound Strep-PE to pSB-biotin beads remained unchanged (see the Supporting Information, Figure S13), indicating saturation of Strep-PE on those beads. The non-Gaussian distribution of the fluorescence intensity of Strep-PE on pSB-biotin beads might be explained by the tetravalent nature of streptavidin. One streptavidin protein might bind to one or multiple biotin moieties on the bead surface.

To demonstrate that the use of pSB-coated Dynabeads is not limited to the "classic" well-known biotin−streptavidin

DOI: 10.1021/acsami.7b09725
ACS Appl. Mater. Interfaces 2017, 9, 38211−38221

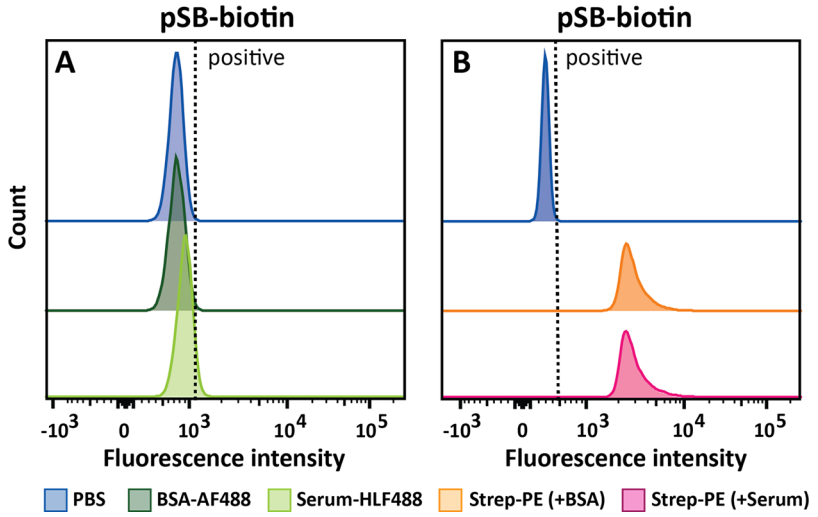

Figure 7. Flow cytometry data of pSB-biotin beads incubated with PBS or a mixture of Strep-PE (50 μg/mL) and either BSA-AF4888 (0.5 mg/mL) or serum-HLF488 (10%, ~6 mg/mL). (A) 488 channel showing BSA-AF488 and serum-HLF488 binding; PBS (blue) and BSA-AF488 (dark green) completely overlap, (B) PE channel showing Strep-PE binding; Strep-PE mixed with BSA-AF488 (orange) completely overlaps with Strep-PE mixed with serum-HLF488 (magenta).

interaction with high affinity, but can also be extended to other more weakly binding interaction partners, we also investigated the ability of pSB beads functionalized with mannose to specifically bind ConA (50 μg/mL) from a mixture with BSA-AF488 or serum-HL488. To this end, pSB beads were functionalized with propargylamine to first install alkyne moieties on the bead surface (Scheme 1, route c3), followed by a CuAAC reaction with mannose-C_{11}-azide (Scheme 1, route d3). Similar to pSB-biotin beads, pSB-mannose beads showed no fouling of BSA-AF488 and only slight protein adsorption when incubated with serum-HLF488. By contrast, ConA-AF365 was specifically bound by the pSB-mannose beads from both protein mixtures (see the Supporting Information, Figure S14), although the same level of fluorescence as for Strep-PE on pSB-biotin beads could not be reached. This could be explained by the weaker interaction between ConA and mannose and/or by a less efficient incorporation of propargylamine or subsequent mannose attachment. Nonetheless, the ability to detect ConA demonstrates the versatility of pSB-coated beads and illustrates their great potential to be used in sensing applications.

We envision that the bead-based platform developed here may serve multiple purposes as a generic tool to (1) study antifouling materials in a quick and scalable manner, (2) investigate the interactions of poorly understood interaction partners, (3) isolate biomolecules (e.g. proteins or cells), and (4) serve as a biosensor system that requires stringent antifouling conditions. Billions of antifouling beads are easily prepared at once, which not only enables good statistics (thousands of beads are typically measured per sample vs 1 chip in e.g. surface plasmon resonance analysis), but also provides an easy and affordable way of screening reaction conditions (e.g. the effect of certain additives on antifouling behavior). Because of the versatility of the beads with regard to functional group installment, this platform would serve well to investigate yet to be identified or poorly understood interaction partners. Tailor-made molecules like sugars or peptides attached to the antifouling beads could, in combination with flow cytometry and other techniques, aid to get a better understanding of interacting biomolecules (e.g. which sugar/glycan is bound by which protein) without background interference. Alternatively, the beads can be used to capture a specific protein, cell, or microbe from a complex pool of other biological entities to be either used as a biosensor platform that requires stringent antifouling conditions or to obtain highly pure biological materials.

CONCLUSION

We present a novel route toward top-functionalized zwitterionic polymer-coated micron-sized beads. These beads show excellent antifouling properties and are able to specifically bind a target protein, even from a complex mixture of serum proteins. Confocal microscopy and flow cytometry measurements both revealed that no nonspecific adsorption of BSA and hardly any adsorption of serum proteins occurred on pSB-coated beads, whereas streptavidin and ConA could be specifically bound to pSB-biotin and pSB-mannose beads, respectively. The ability to discriminate between specific and nonspecific binding on many particles simultaneously, together with the high dynamic range of protein detection, makes flow cytometry an excellent technique to study biofouling on micron-sized beads.

The unique combination of excellent antifouling properties and specific binding of target proteins with a routinely used technique such as flow cytometry, which is used as a read-out system, makes this platform attractive for biosensing applications that require stringent antifouling conditions. Moreover, the versatility of the beads with respect to the installment of functional groups via click chemistry (either SPAAC or CuAAC, with azide or alkyne on the bead) or substituting the terminal halide with an amine of choice also enables these beads to be used for the investigation of a wide range of tailor-made recognition elements.

ASSOCIATED CONTENT

Supporting Information

The Supporting Information is available free of charge on the ACS Publications website at DOI: 10.1021/acsami.7b09725.

Complementary XPS and FT-IR spectra, complementary flow cytometry data including additional data of pSB-

DOI: 10.1021/acsami.7b09725
ACS Appl. Mater. Interfaces 2017, 9, 38211−38221

mannose beads and gating strategy, and complementary ELISA and confocal microscopy images (PDF)

AUTHOR INFORMATION

Corresponding Authors

*E-mail: Huub.Savelkoul@wur.nl (H.F.J.S.).
*E-mail: Han.Zuilhof@wur.nl (H.Z.).

ORCID

Ian de Bus: 0000-0002-1061-8352
Maarten M. J. Smulders: 0000-0002-6855-0426
Han Zuilhof: 0000-0001-5773-8506

Notes

The authors declare no competing financial interest.

ACKNOWLEDGMENTS

The authors thank Ben Meijer and Jan Willem Borst for their assistance with flow cytometry and confocal microscopy, respectively, and Stefanie C. Lange for stimulating discussions along the process of preparing our antifouling beads. This work was supported by NanoNextNL (program 3E), a micro and nanotechnology consortium of the government of The Netherlands and 130 partners.

REFERENCES

(1) Reddy, L. H.; Arias, J. L.; Nicolas, J.; Couvreur, P. Magnetic Nanoparticles: Design and Characterization, Toxicity and Biocompatibility, Pharmaceutical and Biomedical Applications. *Chem. Rev.* **2012**, *112*, 5818−5878.

(2) Haukanes, B.-I.; Kvam, C. Application of Magnetic Beads in Bioassays. *Biotechnology* **1993**, *11*, 60−63.

(3) Morgan, E.; Varro, R.; Sepulveda, H.; Ember, J. A.; Apgar, J.; Wilson, J.; Lowe, L.; Chen, R.; Shivraj, L.; Agadir, A.; Campos, R.; Ernst, D.; Gaur, A. Cytometric Bead Array: A Multiplexed Assay Platform with Applications in Various Areas of Biology. *Clin. Immunol.* **2004**, *110*, 252−266.

(4) Arruebo, M.; Fernández-Pacheco, R.; Ibarra, M. R.; Santamaría, J. Magnetic Nanoparticles for Drug Delivery. *Nano Today* **2007**, *2*, 22−32.

(5) Mornet, S.; Vasseur, S.; Grasset, F.; Veverka, P.; Goglio, G.; Demourgues, A.; Portier, J.; Pollert, E.; Duguet, E. Magnetic Nanoparticle Design for Medical Applications. *Prog. Solid State Chem.* **2006**, *34*, 237−247.

(6) Jia, G.; Cao, Z.; Xue, H.; Xu, Y.; Jiang, S. Novel Zwitterionic-Polymer-Coated Silica Nanoparticles. *Langmuir* **2009**, *25*, 3196−3199.

(7) Yang, W.; Zhang, L.; Wang, S.; White, A. D.; Jiang, S. Functionalizable and Ultra Stable Nanoparticles Coated with Zwitterionic Poly(Carboxybetaine) in Undiluted Blood Serum. *Biomaterials* **2009**, *30*, 5617−5621.

(8) Kim, G.; Yong, Y.; Kang, H. J.; Park, K.; Kim, S. I.; Lee, M.; Huh, N. Zwitterionic Polymer-Coated Immunobeads for Blood-Based Cancer Diagnostics. *Biomaterials* **2014**, *35*, 294−303.

(9) Lin, R.; Li, Y.; MacDonald, T.; Wu, H.; Provenzale, J.; Peng, X.; Huang, J.; Wang, L.; Wang, A. Y.; Yang, J.; Mao, H. Improving Sensitivity and Specificity of Capturing and Detecting Targeted Cancer Cells with Anti-Biofouling Polymer Coated Magnetic Iron Oxide Nanoparticles. *Colloids Surf., B* **2017**, *150*, 261−270.

(10) Schlenoff, J. B. Zwitteration: Coating Surfaces with Zwitterionic Functionality to Reduce Nonspecific Adsorption. *Langmuir* **2014**, *30*, 9625−9636.

(11) Shao, Q.; Jiang, S. Y. Molecular Understanding and Design of Zwitterionic Materials. *Adv. Mater.* **2015**, *27*, 15−26.

(12) Prime, K.; Whitesides, G. Self-Assembled Organic Monolayers: Model Systems for Studying Adsorption of Proteins at Surfaces. *Science* **1991**, *252*, 1164−1167.

(13) Li, L.; Chen, S.; Zheng, J.; Ratner, B. D.; Jiang, S. Protein Adsorption on Oligo(Ethylene Glycol)-Terminated Alkanethiolate Self-Assembled Monolayers: The Molecular Basis for Nonfouling Behavior. *J. Phys. Chem. B* **2005**, *109*, 2934−2941.

(14) Ostuni, E.; Chapman, R. G.; Holmlin, R. E.; Takayama, S.; Whitesides, G. M. A Survey of Structure−Property Relationships of Surfaces that Resist the Adsorption of Protein. *Langmuir* **2001**, *17*, 5605−5620.

(15) Li, L.; Chen, S.; Jiang, S. Protein Interactions with Oligo-(Ethylene Glycol) (Oeg) Self-Assembled Monolayers: Oeg Stability, Surface Packing Density and Protein Adsorption. *J. Biomater. Sci., Polym. Ed.* **2007**, *18*, 1415−1427.

(16) Ladd, J.; Zhang, Z.; Chen, S.; Hower, J. C.; Jiang, S. Zwitterionic Polymers Exhibiting High Resistance to Nonspecific Protein Adsorption from Human Serum and Plasma. *Biomacromolecules* **2008**, *9*, 1357−1361.

(17) Vaisocherová, H.; Zhang, Z.; Yang, W.; Cao, Z.; Cheng, G.; Taylor, A. D.; Piliarik, M.; Homola, J.; Jiang, S. Y. Functionalizable Surface Platform with Reduced Nonspecific Protein Adsorption from Full Blood Plasma—Material Selection and Protein Immobilization Optimization. *Biosens. Bioelectron.* **2009**, *24*, 1924−1930.

(18) Nguyen, A. T.; Baggerman, J.; Paulusse, J. M. J.; van Rijn, C. J. M.; Zuilhof, H. Stable Protein-Repellent Zwitterionic Polymer Brushes Grafted from Silicon Nitride. *Langmuir* **2011**, *27*, 2587−2594.

(19) Kim, J. C.; Kim, M.; Jung, J.; Kim, H.; Kim, I. J.; Kim, J. R.; Ree, M. Biocompatible Characteristics of Sulfobetaine-Containing Brush Polymers. *Macromol. Res.* **2012**, *20*, 746−753.

(20) Matyjaszewski, K.; Xia, J. Atom Transfer Radical Polymerization. *Chem. Rev.* **2001**, *101*, 2921−2990.

(21) Jiang, S.; Cao, Z. Ultralow-Fouling, Functionalizable, and Hydrolyzable Zwitterionic Materials and Their Derivatives for Biological Applications. *Adv. Mater.* **2010**, *22*, 920−932.

(22) Zhang, Z.; Vaisocherová, H.; Cheng, G.; Yang, W.; Xue, H.; Jiang, S. Nonfouling Behavior of Polycarboxybetaine-Grafted Surfaces: Structural and Environmental Effects. *Biomacromolecules* **2008**, *9*, 2686−2692.

(23) Ning, J.; Li, G.; Haraguchi, K. Synthesis of Highly Stretchable, Mechanically Tough, Zwitterionic Sulfobetaine Nanocomposite Gels with Controlled Thermosensitivities. *Macromolecules* **2013**, *46*, 5317−5328.

(24) Pochechueva, T.; Chinarev, A.; Bovin, N.; Fedier, A.; Jacob, F.; Heinzelmann-Schwarz, V. Pegylation of Microbead Surfaces Reduces Unspecific Antibody Binding in Glycan-Based Suspension Array. *J. Immunol. Methods* **2014**, *412*, 42−52.

(25) Kim, G.; Yoo, C. E.; Kim, M.; Kang, H. J.; Park, D.; Lee, M.; Huh, N. Noble Polymeric Surface Conjugated with Zwitterionic Moieties and Antibodies for the Isolation of Exosomes from Human Serum. *Bioconjugate Chem.* **2012**, *23*, 2114−2120.

(26) Shapiro, H. M. *Practical Flow Cytometry*, 4th ed.; WILEY-LISS: Hoboken, NJ, 2003.

(27) Jahan-Tigh, R. R.; Ryan, C.; Obermoser, G.; Schwarzenberger, K. Flow Cytometry. *J. Invest. Dermatol.* **2012**, *132*, 1−6.

(28) Barlogie, B.; Raber, M. N.; Schumann, J.; Johnson, T. S.; Drewinko, B.; Swartzendruber, D. E.; Göhde, W.; Andreeff, M.; Freireich, E. J. Flow Cytometry in Clinical Cancer Research. *Cancer Res.* **1983**, *43*, 3982−3997.

(29) Lange, S. C.; van Andel, E.; Smulders, M. M. J.; Zuilhof, H. Efficient and Tunable Three-Dimensional Functionalization of Fully Zwitterionic Antifouling Surface Coatings. *Langmuir* **2016**, *32*, 10199−10205.

(30) Debrassi, A.; Ribbera, A.; de Vos, W. M.; Wennekes, T.; Zuilhof, H. Stability of (Bio)Functionalized Porous Aluminum Oxide. *Langmuir* **2014**, *30*, 1311−1320.

(31) Pujari, S. P.; Spruijt, E.; Stuart, M. A. C.; van Rijn, C. J. M.; Paulusse, J. M. J.; Zuilhof, H. Ultralow Adhesion and Friction of Fluoro-Hydro Alkyne-Derived Self-Assembled Monolayers on H-Terminated Si(111). *Langmuir* **2012**, *28*, 17690−17700.

(32) Debrassi, A.; Roeven, E.; Thijssen, S.; Scheres, L.; de Vos, W. M.; Wennekes, T.; Zuilhof, H. Versatile (Bio)Functionalization of

DOI: 10.1021/acsami.7b09725
ACS Appl. Mater. Interfaces 2017, 9, 38211−38221

Bromo-Terminated Phosphonate-Modified Porous Aluminum Oxide. *Langmuir* **2015**, *31*, 5633−5644.
(33) Li, Y.; Giesbers, M.; Gerth, M.; Zuilhof, H. Generic Top-Functionalization of Patterned Antifouling Zwitterionic Polymers on Indium Tin Oxide. *Langmuir* **2012**, *28*, 12509−12517.
(34) Hong, V.; Presolski, S. I.; Ma, C.; Finn, M. G. Analysis and Optimization of Copper-Catalyzed Azide−Alkyne Cycloaddition for Bioconjugation. *Angew. Chem., Int. Ed.* **2009**, *48*, 9879−9883.
(35) Blaszykowski, C.; Sheikh, S.; Thompson, M. Surface Chemistry to Minimize Fouling from Blood-Based Fluids. *Chem. Soc. Rev.* **2012**, *41*, 5599−5612.
(36) Yang, W.; Chen, S.; Cheng, G.; Vaisocherová, H.; Xue, H.; Li, W.; Zhang, J.; Jiang, S. Film Thickness Dependence of Protein Adsorption from Blood Serum and Plasma onto Poly(Sulfobetaine)-Grafted Surfaces. *Langmuir* **2008**, *24*, 9211−9214.
(37) Riedel, T.; Riedelová-Reicheltová, Z.; Májek, P.; Rodriguez-Emmenegger, C.; Houska, M.; Dyr, J. E.; Brynda, E. Complete Identification of Proteins Responsible for Human Blood Plasma Fouling on Poly(Ethylene Glycol)-Based Surfaces. *Langmuir* **2013**, *29*, 3388−3397.
(38) Nguyen, A. T.; Baggerman, J.; Paulusse, J. M. J.; Zuilhof, H.; van Rijn, C. J. M. Bioconjugation of Protein-Repellent Zwitterionic Polymer Brushes Grafted from Silicon Nitride. *Langmuir* **2012**, *28*, 604−610.
(39) Cai, Y.; Schwartz, D. K. Influence of Protein Surface Coverage on Anomalously Strong Adsorption Sites. *ACS Appl. Mater. Interfaces* **2016**, *8*, 511−520.
(40) Langdon, B. B.; Kastantin, M.; Walder, R.; Schwartz, D. K. Interfacial Protein−Protein Associations. *Biomacromolecules* **2014**, *15*, 66−74.

DOI: 10.1021/acsami.7b09725
ACS Appl. Mater. Interfaces 2017, 9, 38211−38221